Lentivirus-mediated transfer of gene encoding fibroblast growth factor-18 inhibits intervertebral disc degeneration

SHENG LU and CHAO-WEI LIN

Department of Spine Surgery, The First Affiliated Hospital of Wenzhou Medical University, Wenzhou, Zhejiang 325000, P.R. China

Received September 17, 2020; Accepted April 23, 2021

DOI: 10.3892/etm.2021.10288

Abstract. Fibroblast growth factor 18 (FGF-18) is a well-characterized anabolic growth factor involved in cartilage homeostasis. However, the effect of FGF-18 on intervertebral disc (IVD) degeneration has not been investigated. The present study aimed to investigate the role of FGF-18 in the process of rabbit IVD degeneration. *In vitro*, primary nucleus pulposus cells (NPs) were cultured and transfected with a lentivirus. Tert-butyl hydroperoxide (TBHP) was used to induce apoptosis in NPs on the second passage, while overexpression of FGF-18 in NPs attenuated TBHP-induced apoptosis. A rabbit annular puncture model was generated to induce IVD degeneration *in vivo*. The discs were injected with an FGF-18-overexpression lentivirus or a negative control lentivirus. In the sham group, the discs were exposed and not punctured. Disc degeneration was evaluated using H&E staining and a histological grading system. Reverse transcription-quantitative PCR was used to detect the expression of the extracellular matrix-degrading enzymes matrix metalloproteinase-3 (MMP-3) and A disintegrin and metalloproteinase with thrombospondin motifs 5 (ADAMTS-5). Nucleus pulposus apoptosis was detected via western blotting, immunohistochemical methods and TUNEL staining. Histologic examination showed that disc degeneration was attenuated after FGF-18 overexpression treatment. At 8 weeks after surgery, the expression of MMP-3 and ADAMTS-5 in the annular puncture groups was higher compared with in the sham group. FGF-18 treatment inhibited the expression of MMP-3 and ADAMTS-5 at the mRNA level. Western blot assays indicated that the expression level of Bax was significantly reduced in the FGF-18 groups, and that the expression level of Bcl-2 was significantly increased compared with those in the control group. Moreover, immunohistochemical analysis indicated that the FGF-18 group exhibited a lower percentage of cleaved caspase 3-positive NPs. Quantification of the TUNEL staining demonstrated that the FGF-18 group had fewer apoptotic NPs than the control group. These findings indicated that FGF-18 could delay IVD degeneration by inhibiting the apoptosis of NPs and the expression of matrix-degrading enzymes.

Correspondence to: Dr Chao-Wei Lin, Department of Spine Surgery, The First Affiliated Hospital of Wenzhou Medical University, Nanbaixiang Street, Wenzhou, Zhejiang 325000, P.R. China
E-mail: 280399040@qq.com

Key words: lentivirus, intervertebral disc degeneration, fibroblast growth factor 18, extracellular matrix-degrading enzyme, apoptosis

Introduction

Intervertebral disc (IVD) degeneration is the leading cause of chronic back pain, which impairs daily quality of life (1). Until recent developments, conservative treatment or surgical procedures were the only strategies put in place to ameliorate the clinical symptoms, due to poor understanding of the pathophysiology of IVD degeneration (2). The major goals of numerous studies include the development of etiological treatments and the reversal of the degeneration process (3).

An increasing number of recent studies have shown that growth factors play important roles in the occurrence and development of IVD degeneration (4-6). Growth factors constitute a group of low molecular weight proteins involved in mitosis and the stimulation of the synthesis of extracellular matrix (1,7). Various growth factors, such as insulin-like growth factor (IGF), TGF-β and bone morphogenetic proteins, have been identified as anabolic regulators that alter homeostasis by shifting the cellular metabolism to the anabolic state in IVD (8-10).

Members of the fibroblast growth factor (FGF) family have been shown to contribute to the regulation of articular and IVD homeostasis (11,12). FGF-18 has been identified as an anabolic growth factor involved in cartilage homeostasis (13). A single intravenous injection of pharmacologic doses of FGF-18 can stimulate the expansion of various cartilage depots in rats, including the rib-sternum junction, trachea, spine and articular cartilage, within 2 weeks (14). In a rat osteoarthritis model, a series of FGF-18 intra-articular injections was able to increase cartilage formation and reduce cartilage degeneration in the tibial plateau (15). However, the role of FGF-18 in IVD degeneration has not been investigated.

IVD degeneration is a chronic process; hence, a single injection may not achieve satisfactory therapeutic effect because the half-life of FGF-18 in the nucleus pulposus is unknown (16). Prolonged exposure to growth factors may be

needed to stimulate biological repair. Gene therapy techniques have been used to explore the effects of growth factors on IVD (17,18). In the present study, a lentivirus-mediated gene transfer approach was used to investigate the effect of FGF-18 treatment on IVD degeneration in a rabbit model. In addition, tert-butyl hydroperoxide (TBHP) was used to induce the apoptosis of nucleus pulposus cells (NPs), and the protective effects of FGF-18 overexpression were evaluated *in vitro*.

The purpose of the present study was to perform a preliminarily assessment of the application of FGF-18 for the treatment of IVD degeneration. The effects of the lentivirus-mediated delivery of FGF-18 on IVD degeneration were evaluated in a puncture-induced IVD degeneration *in vivo* model in rabbits and in TBHP-treated NP cells *in vitro*. The results suggested that FGF-18 can delay IVD degeneration by inhibiting the apoptosis of NPs and the expression of matrix-degrading enzymes.

Materials and methods

Animals. Adult New Zealand 45 female white rabbits (age, 21-23 weeks; weight, 3.0-3.5 kg) were purchased from Experimental Animal Center of Wenzhou Medical University (license no. SYXK(Zhe)2010-0150). All procedures and experimental operations were approved by the Animal Care and Use Committee of Wenzhou Medical University and conformed to the Guide for the Care and Use of Laboratory Animals of the National Institutes of Health (19).

Reagents and antibodies. TBHP and type II collagenase were obtained from Sigma-Aldrich; Merck KGaA. Rabbit anti-FGF-18 antibody was purchased from LifeSpan Biosciences. Mouse monoclonal anti-Bcl-2 (cat. no. ab692) and anti-Bax (cat. no. ab3191) antibodies were purchased from Abcam. Mouse monoclonal anti-GAPDH antibody (cat. no. #51332), rabbit monoclonal anti-cleaved caspase-3 antibody (cat. no. #9664), goat anti-rabbit IgG-HRP (cat. no. #7047) and goat anti-mouse IgG-HRP (cat. no. #7076) were purchased from Cell Signaling Technology, Inc. Mouse monoclonal anti-Flag antibody (cat. no. F3165) was purchased from Sigma-Aldrich; Merck KGaA. An *in situ* cell death detection kit, POD (cat. no. 11684817910) was purchased from Roche Diagnostics.

Lentiviral vector construction and lentivirus production. The rabbit FGF-18 sequence was obtained from the NCBI database (https://www.ncbi.nlm.nih.gov/nuccore/XM_002710377.3). A Ubi-MCS-3FLAG-SV40-EGFP vector (Gv287 backbone; Shanghai GeneChem Co., Ltd.) was linearized using the *Age*I restriction enzyme (New England BioLabs, Inc.). To create the recombinant Ubi-LV vector, a fragment containing FGF-18 was constructed into the GV287 vector. Then, the recombinant Ubi-LV vector was transformed into 293T cells [(cultured in DMEM (Gibco; Thermo Fisher Scientific, Inc.), containing 10% FBS (Gibco; Thermo Fisher Scientific, Inc.), 100 U/ml penicillin and 100 μg/ml streptomycin, and placed at 37˚C in a humidified incubator containing 5% CO_2)]. After identification by PCR and sequencing (data not shown), the 20 μg Ubi-LV vector in combination with the lentiviral packaging vectors (15 μg pHelper1.0 and 20 μg pHelper2.0) (Shanghai GeneChem Co., Ltd.) were transfected into 293T cells, using Lipofectamine® 2000 (Invitrogen; Thermo Fisher Scientific, Inc.) to generate the virus. The virus titer was determined using the gradient dilution method (20).

NP culture and viability assay. Rabbits were euthanized with an overdose of 10% sodium pentobarbital (100 mg/kg) via intravenous injection. Death was verified by cessation of the heartbeat and lack of movement. The gel-like nucleus pulposus tissue was separated from the anulus fibrosus under a dissection microscope, and the tissue was treated with 0.1% collagenase and 2 U/ml hyaluronidase for 4 h at 37˚C. Subsequently, the digested tissue was transferred as explants cultured in DMEM (Gibco; Thermo Fisher Scientific, Inc.) supplemented with 10% heat-inactivated FBS (Gibco; Thermo Fisher Scientific, Inc.) and antibiotics (100 U/ml penicillin and 100 μg/ml streptomycin) in a humidified atmosphere containing 5% CO_2 at 37˚C. The NPs separated from the explant culture after 1 week. Confluent cells were harvested by using 0.25% trypsin-EDTA solution and sub-cultured in 10-cm dishes or 6-well plates. When reaching 20-30% confluence, corresponding to the stage with optimal infection efficiency, the cells at first passage were infected with various concentrations of lentivirus (with MOI ranging from 1-100). Fluorescent protein expression in the cells was observed using an inverted fluorescence microscope (Nikon Corporation) at 24, 48 and 72 h post-infection to assess the infection efficiency. After a second passage, the cells were treated with TBHP at various concentration (0, 50, 100, 200, 300, 500 μM) for 4 h at 37˚C. Then, cell viability was determined by Cell Counting Kit-8 (CCK-8; Dojindo Molecular Technologies, Inc.) at 37˚C for 2 h, according to the manufacturer's instructions.

Animal model and lentivirus-mediated gene transfer. A rabbit annular puncture model (5 rabbits/group) was generated to induce IVD degeneration at L3/4, L4/5 and L5/6 (21). All animals were anesthetized intraperitoneally with 2% (w/v) pentobarbital (40 mg/kg). After puncture, ~10^9 PFU of the FGF-18 overexpression lentivirus were injected into the center of the rabbit nucleus pulposus using a 100-μl micro-syringe (Hamilton Company) along the initial foramina. Negative control lentivirus with no gene overexpression was injected in the control group. In the sham group, IVDs were only exposed and were not punctured.

Histologic and immunohistochemical analysis. At 8 weeks after surgery, the rabbits were sacrificed via an intravenous injection of 10% sodium pentobarbital (100 mg/kg). The IVDs were separated, fixed in 10% neutral buffered formalin at 4˚C for 3 days and decalcified in the presence of 10% EDTA for 2-6 weeks. The samples were incubated in a mixture of xylene and paraffin at 25˚C for 15 min, and paraffin I and paraffin II were then added for 50-60 min each. The tissue was subsequently sliced into 5-μm-thick sections. For H&E staining, the sections were washed three times with PBS for 5 min each. and incubated with hematoxylin for 5 min and eosin for another 5 min at room temperature. After three more 5-min washes with PBS, the sections were dehydrated in 95% alcohol, permeabilized with xylene and mounted with

Table I. Primer sequences used for reverse transcription-quantitative PCR.

Gene	Primer	Sequence	Size, bp
MMP3	Forward	5'-CCCAAAGTGGACAAAAACTCA-3'	118
	Reverse	5'-AGTCACCTCCTCCCAGACCT-3'	
ADAMTS-5	Forward	5'-GTGGAGTATGCGGAGGAGAC-3'	139
	Reverse	5'-TCTTTGGCTTTGAACTGTCG -3'	
GAPDH	Forward	5'-TGAACGGGAAACTCACTGG-3'	117
	Reverse	5'-TCACCACCTTCTTGATGTCG-3'	

MMP-3, matrix metalloproteinase-3; ADAMTS-5, A disintegrin and metalloproteinase with thrombospondin motifs 5.

neutral resin. A widely used grading scale was subsequently used to assess the anulus fibrosus, the border between the anulus fibrosus and nucleus pulposus, the cellularity of the nucleus purpose and the matrix of the nucleus pulposus (14). Grades ranged from 4 to 12, where 'normal' is 1 point for each of the four categories listed above, for a total of four points (grade 4). Since there is a maximum of three points for each parameter, a total of 12 points (grade 12) is representative of severe degeneration (20). A grading system was used to evaluate semi-quantitatively disc degeneration as previously described (22).

Immunohistochemical staining for cleaved caspase-3 was performed using the sections obtained 8 weeks after the operation. After incubation with 3% H_2O_2 at room temperature for 10 min, the tissue was washed with PBS, boiled in 0.1% trisodium citrate at 90˚C for 15 min for antigen retrieval and blocked with BSA (cat. no. 4240GR100; NeoFroxx GmbH) at room temperature for 1 h. Subsequently, the sections were incubated with a rabbit anti-cleaved caspase-3 monoclonal antibody (1:200) diluted in PBS overnight at 4˚C, followed by an incubation with HRP-conjugated secondary antibodies (1:1,000) for 1 h at room temperature. The staining was visualized with 3,3'-diaminobenzidine (OriGene Technologies, Inc.), and the sections were counterstained with hematoxylin at room temperature for 1 min, dehydrated with graded ethanol, clarified with dimethylbenzene and sealed with neutral resin. Images (magnification, x200) were acquired using a light imaging microscope (BX53; Olympus Corporation), and the percentage of cleaved caspase-3-positive cells in five randomly selected fields per sample was determined, and the images were analyzed by ImageJ v1.44 software (National Institutes of Health).

TUNEL assay. TUNEL assay was performed to detect DNA fragmentation induced by apoptotic signaling cascades. Transverse sections prepared as aforementioned were washed with distilled water and incubated with protein digestion enzyme K for 20 min at 37˚C. Then, the *in situ* cell death detection kit, POD (Roche Diagnostics) was used for the TUNEL assay according to the manufacturer's instructions. Sections were stained with DAPI (1:1,000; MilliporeSigma) at room temperature for 10 min to visualize the nucleus. Images were evaluated using a fluorescence microscope (DP70; Olympus Corporation) at x200 magnification, the percentage of positive cells was quantified in five randomly selected fields per sample, and the images were analyzed using ImageJ v1.44 software (National Institutes of Health).

Reverse transcription-quantitative PCR (RT-qPCR) analysis. Total RNA was extracted from the nucleus pulposus using TRIzol® reagent (Invitrogen; Thermo Fisher Scientific, Inc.) and then RNA was reversely transcribed into cDNA with a SuperScript™ One-Step Reverse Transcription kit (Invitrogen; Thermo Fisher Scientific, Inc.), according to the manufacturer's instructions. The mRNA expression of matrix metalloproteinase-3 (MMP-3) and A disintegrin and metalloproteinase with thrombospondin motifs 5 (ADAMTS-5) were quantified using the iTaq™ Universal SYBR-Green Supermix (Bio-Rad Laboratories, Inc.) on the Real-Time PCR detection System (Applied Biosystems; Thermo Fisher Scientific, Inc.). The thermocycling conditions used were as follows: 95˚C for 10 min, followed by 40 cycles of 95˚C for 15 sec, 60˚C for 30 sec and 72˚C for 30 sec. Samples were amplified independently at least three times. Relative gene expression was converted using the $2^{-\Delta\Delta Cq}$ method against GAPDH (23). All primer sequences were designed and synthesized by Sangon Biotech Co. Ltd. and are presented in Table I.

Western blot analysis. The nucleus pulposus tissues or cultured cells were lysed in ice-cold RIPA buffer (cat. no. P0013B; Beyotime Institute of Biotechnology), 100 mM Na_3VO_4, 100 mM NaF, 100 mM PMSF (cat. no. ST506; Beyotime Institute of Biotechnology) at 4˚C for 30 min, then centrifuged at 12,000 x g for 30 min at 4˚C, and protein concentration was determined using the BCA method (Pierce BCA Protein Assay kit; Thermo Fisher Scientific, Inc.). Finally, lysates were mixed with 5X loading buffer (cat. no. P1040; Beijing Solarbio Science & Technology Co., Ltd.) and boiled at 100˚C for 10 min. The equivalent of 20 μg of protein was separated via 12% SDS-PAGE and then transferred onto a PVDF membrane (MilliporeSigma). The membranes were blocked with 5% non-fat milk at room temperature for 1 h and then incubated overnight at 4˚C with anti-Flag (1:800), anti-Bcl-2 (1:1,000), anti-Bax (1:1,000) and anti-GAPDH (1:1,000) antibodies. After the membranes were washed with TBS-Tween-20 (0.1%), HRP-conjugated antibodies (1:5,000) was added to develop the signal at room temperature for 1.5 h. Immunoreactive proteins were visualized using an ECL detection kit (Bio-Rad Laboratories, Inc.) and blots were analyzed using Quantity One software v4.6.2 (Bio-Rad Laboratories, Inc.).

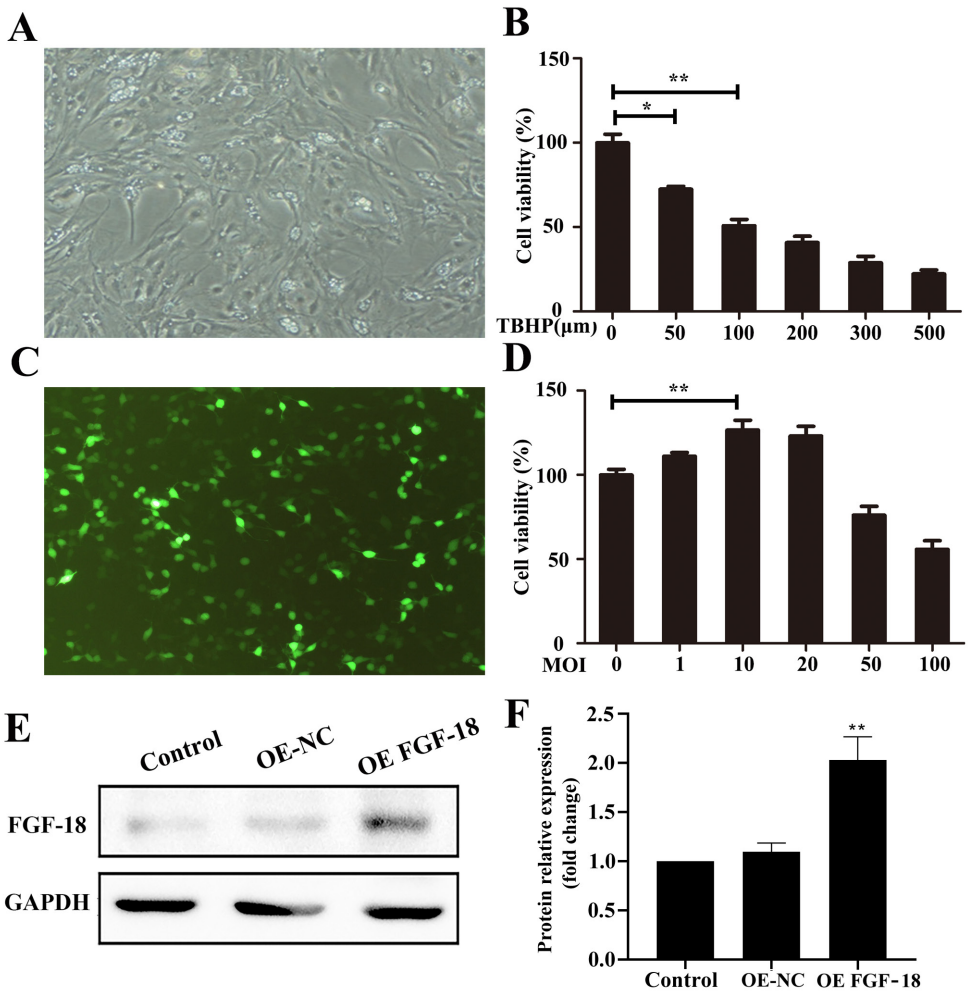

Figure 1. Overexpression of FGF-18 increases viability of NPs. (A) Culture of primary NPs. (B) CCK-8 assay results of NPs treated with various concentrations of TBHP for 4 h. (C) Green fluorescent protein expression in NPs infected with the lentiviruses. (D) CCK-8 assay results of NPs treated with various concentrations of lentivirus for 72 h. (E) Western blot analysis and (F) Fold-change of FGF-18 protein expression. Sham refers to non-transduced cells, control refers to empty vector-expressing lentiviruses. Data are presented as the mean ± SD. *P<0.05, **P<0.01 vs. the indicated groups or OE-NC. NPs, nucleus pulposus cells; TBHP, tert-butyl hydroperoxide; CCK-8, Cell Counting Kit-8; OE, overexpression; NC, negative control; FGF-18, fibroblast growth factor 18.

Statistical analysis. The results are presented as the mean ± SD unless specified otherwise. All experiments were repeated at least three times. Statistical significance was evaluated by using Student's t-test, or comparison between multiple groups was assessed using one-way ANOVA followed by Tukey's post hoc test. For histological grades, data are expressed as a median (interquartile range) and the Kruskal-Wallis test with Dunn's post hoc test was applied to compare multiple groups. SPSS 22.0 (IBM Corp.) and GraphPad Prism 7.0 software (GraphPad Software, Inc.) were used to perform analyses. P<0.05 was considered to indicate a statistically significant difference.

Results

Overexpression of FGF-18 inhibits apoptosis in NPs in vitro. Pre-confluent NPs (Fig. 1A) were transfected with various concentrations of lentivirus (with MOI ranging from 1-100). Cells in green indicated successful transfection (Fig. 1C). CCK-8 assay results indicated that lentiviral transfection at concentrations ≤20 MOI improved cell viability after 72 h (Fig. 1D). However, cell viability was decreased by TBHP treatment in a dose-dependent manner (Fig. 1B). The transfection efficiency *in vitro* was confirmed with quantification of FGF-18 expression in NPs via western blotting (Fig. 1E and F).

FGF-18 overexpression significantly protected NPs against TBHP-induced cell death (Fig. 2A). The expression levels of Bax and Bcl-2 were detected using western blot analyses (Fig. 2B). The results indicated that 100 μM TBHP markedly increased the expression of an apoptosis-related protein (Bax) and decreased the expression of an anti-apoptotic protein (Bcl-2), whereas overexpression of FGF-18 inhibited TBHP-induced apoptosis (Fig. 2C and D).

Anti-catabolic and anti-apoptotic effects of FGF-18 on NPs in vivo. To evaluate the transfection efficiency of FGF-18 overexpression lentivirus in NPs, western blot analysis of exogenous Flag protein was performed. The Flag protein was designed to be co-expressed with FGF-18 and was not expressed in non-infected NPs. As presented in Fig. 3A, the protein level of Flag in rabbit NPs was increased 8 weeks after they were transfected with FGF-18 overexpression lentivirus, whereas it was not detected in the sham or control group.

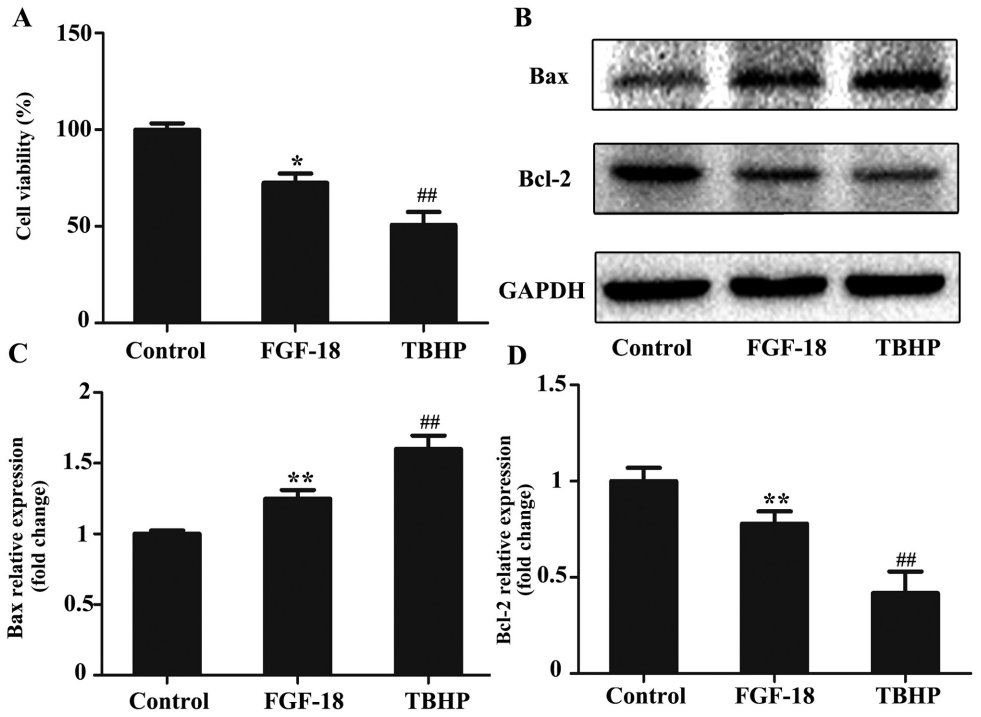

Figure 2. Overexpression of FGF-18 inhibits the apoptosis of NPs. (A) Cell Counting Kit-8 assay results of different groups treated with TBHP (100 μM) for 4 h. (B) Western blot analysis and fold-change of (C) Bax and (D) Bcl-2 in NPs treated with TBHP. Data are presented as the mean ± SD. $^{\#\#}$P<0.01 vs. control; *P<0.05 and **P<0.01 vs. TBHP. NPs, nucleus pulposus cells; TBHP, tert-butyl hydroperoxide; FGF-18, fibroblast growth factor 18.

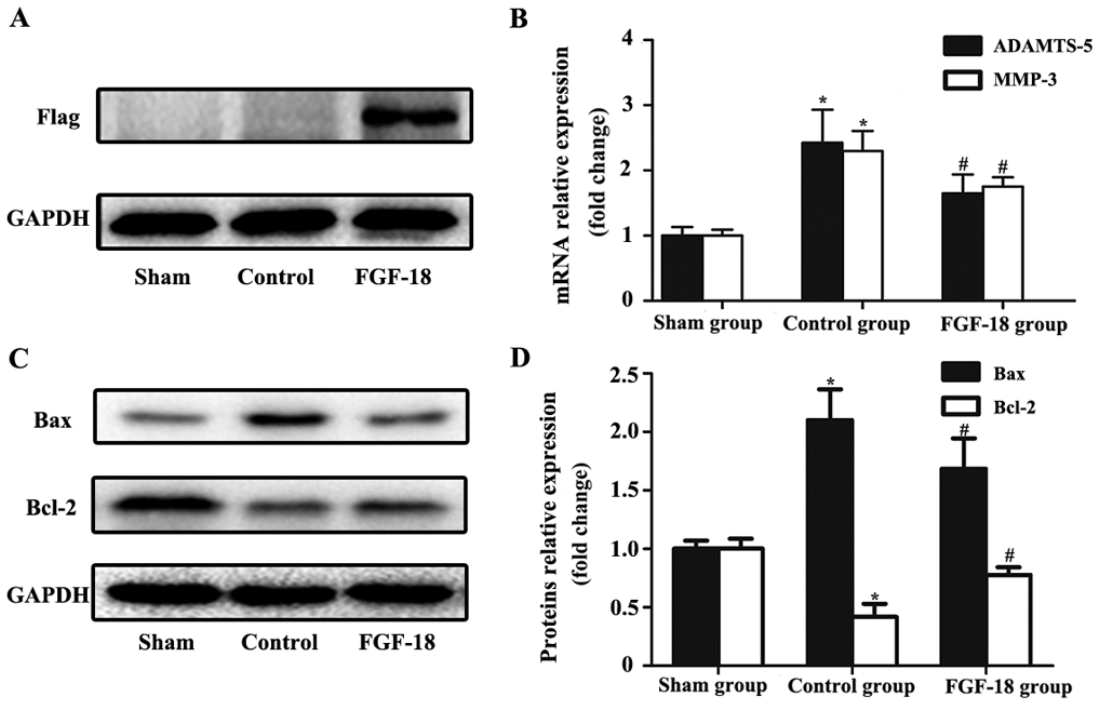

Figure 3. Anti-catabolic and anti-apoptotic effect of FGF-18 on NPs *in vivo*. (A) Western blot assay of Flag protein. (B) Reverse transcription-quantitative PCR analysis of the mRNA expression of ADAMTS-5 and MMP-3 in NPs (n=5). (C) Representative western blot showing the protein expression levels of Bcl-2 and Bax. (D) Statistical analysis of the Bcl-2 and Bax protein expression levels. The band intensities were normalized to GAPDH (n=15). Data are presented as the mean ± SD. *P<0.05 vs. sham; $^{\#}$P<0.05 vs. control. NPs, nucleus pulposus cells; FGF-18, fibroblast growth factor 18; MMP-3, matrix metalloproteinase-3; ADAMTS-5, A disintegrin and metalloproteinase with thrombospondin motifs 5.

RT-qPCR results demonstrated that the mRNA levels of the pro-catabolic indicators MMP-3 and ADAMTS-5 in the control group were markedly increased compared with the sham group (Fig. 3B). FGF-18 treatment decreased the expression levels of both MMP-3 and ADAMTS-5 at the mRNA level compared with the control group (Fig. 3B). As indicated by western blot

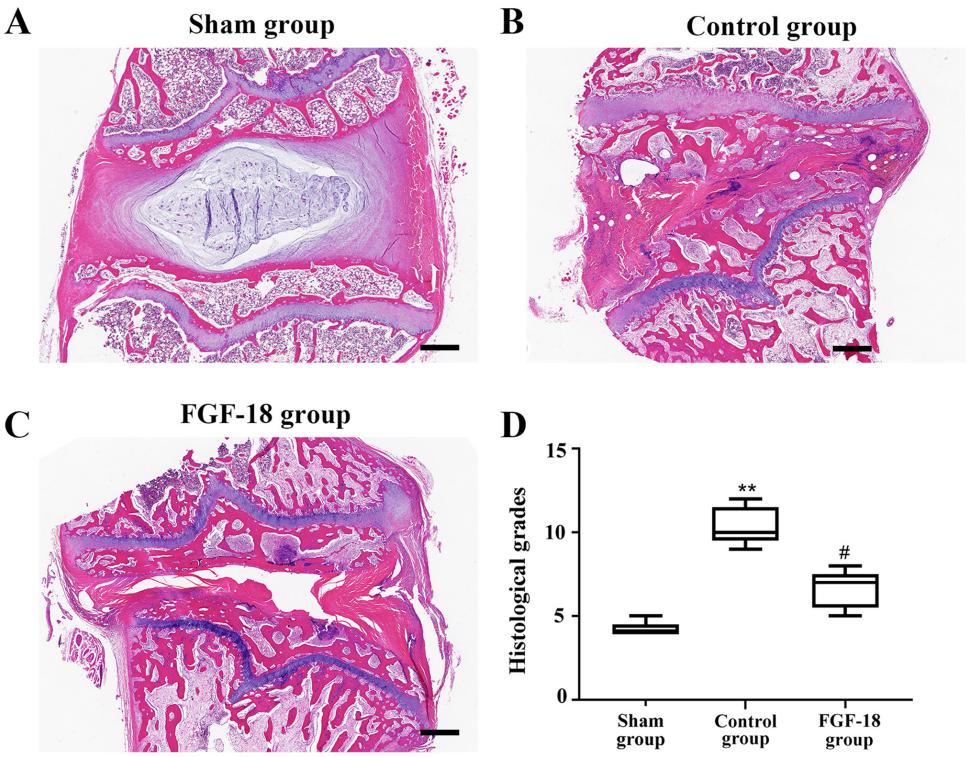

Figure 4. H&E staining of intervertebral discs. Samples of (A) sham, (B) control and (C) FGF-18 groups. Scale bar =20 mm. (D) Semiquantitative histological scores at 8 weeks after the injection. Bars show the median ± interquartile range of 15 discs from five rabbits in each treatment group. **P<0.01 vs. sham group; $^{\#}$P<0.05 vs. control group. FGF-18, fibroblast growth factor 18.

analysis, the expression levels of Bax in the FGF-18 group were significantly reduced compared with those in the control group, and the expression level of Bcl-2 was increased in the FGF-18 group compared with the control group (Fig. 3C and D).

Histologic examination of the rabbit discs after transfer of the FGF-18 overexpression lentivirus. H&E-stained IVDs were observed 8 weeks after the operation (Fig. 4). Abnormalities, such as inflammation or cancerous growth, were not detected in any of the groups. However, after 8 weeks, NPs of the control group had collapsed. As illustrated in Fig. 4B, the destruction structure was accompanied by the absence of vacuoles and fewer NPs, and the space was filled with a hypocellular fibrocartilaginous matrix. By contrast, the rabbits treated with the FGF-18 overexpression lentivirus exhibited numerous large vacuolated cells and smaller chondrocyte-like cells, and the structure was more complete as observed in Fig. 4C. The histological grades in the control group were significantly higher compared with in the sham group (Fig. 4D), and they were significantly lower in the FGF-18 group compared with in the control group (Fig. 4D).

Immunohistochemical analysis of cleaved caspase-3 in rabbit NPs. Immunohistochemical analysis of the *in vivo* experiment indicated that the number of cleaved caspase-3-positive NPs (brown positive signal) was decreased in the sham group. The expression of cleaved caspase-3 in the control group was significantly increased 8 weeks after surgery (Fig. 5A and B). However, the percentage of cleaved caspase-3-positive cells in the FGF-18 group was reduced compared with that in the control group (Fig. 5C).

FGF-18 reduces the NP apoptosis rate. TUNEL staining was performed to analyze the NP apoptosis rate. The apoptosis rate of NPs was increased over time in the control and FGF-18 groups. However, the apoptosis rate was decreased for the FGF-18 group (Fig. 6A). Quantification of TUNEL staining showed that the FGF-18 group exhibited significantly fewer apoptotic NPs compared with the control group (Fig. 6B).

Discussion

The present study suggested that FGF-18 overexpression can delay the process of IVD degeneration. FGF-18 was involved in the protection of NPs against apoptosis, and may suppress extracellular matrix degeneration and promote extracellular matrix synthesis. The results of the *in vivo* experiments indicated that FGF-18 may ameliorate the process of IVD degeneration in a puncture-induced rabbit model. However, the exact mechanism via which FGF-18 attenuates the apoptosis of NPs remains unclear. Further research will be performed to determine the detailed mechanism.

Previous studies have indicated that biological treatments can be used to stimulate cell activity, increase the synthesis of extracellular matrix and reverse the process of IVD degeneration (24). For instance, injection of bone morphogenetic protein-7 into IVDs induced an increase in the height of IVDs (22). In addition, Nishida *et al* (25) reported that the injection of an adenovirus construct encoding TGF-β into lumbar discs may induce proteoglycan (PG) synthesis in rabbits. Interestingly, the gene transfer of tissue inhibitor of metalloproteinases 1, an inhibitor of catabolic enzymes, also increased the PG content in the pellet cultures of human

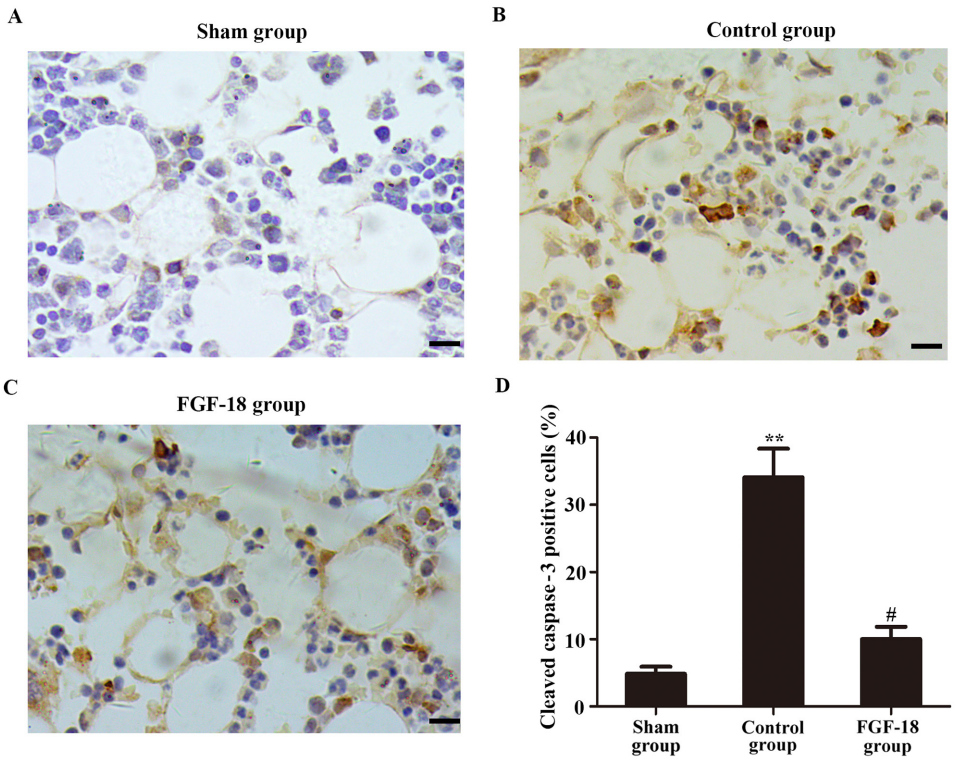

Figure 5. Immunostaining of cleaved caspase-3 in nucleus pulposus cells. Staining in (A) sham, (B) control and (C) FGF-18 groups at 8 weeks after the operation. Scale bar =20 μm. (D) Quantification of cleaved caspase-3-positive cells (n=5). Data are presented as the mean ± SD. **P<0.01 vs. sham; $^{\#}$P<0.05 vs. control. FGF-18, fibroblast growth factor 18.

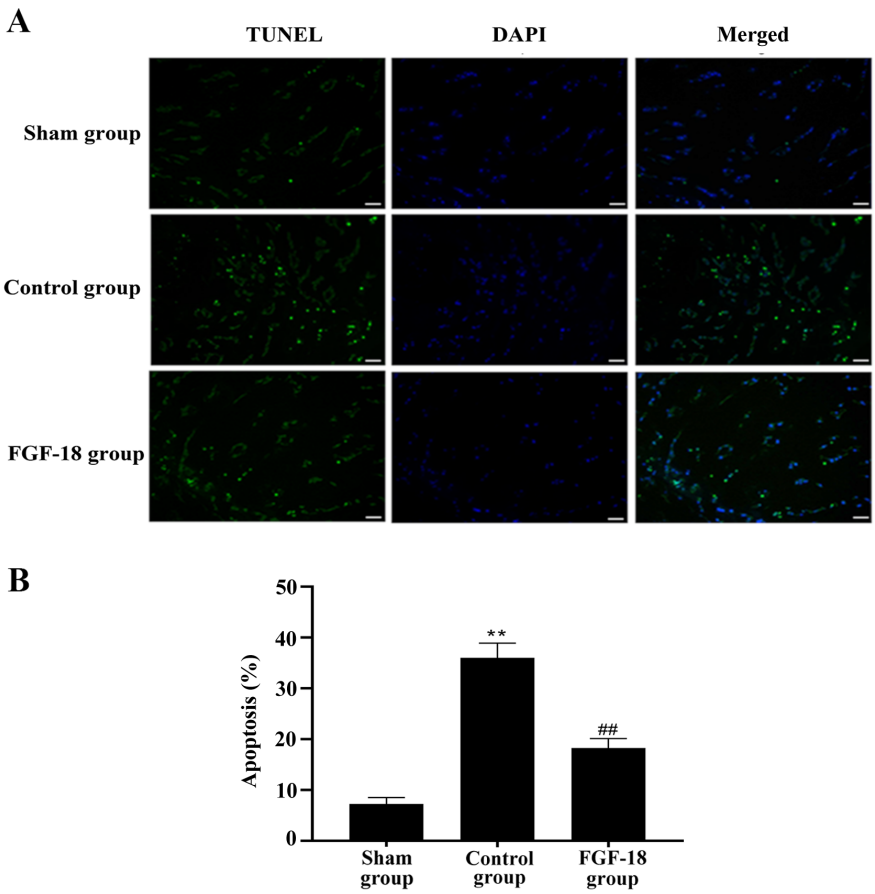

Figure 6. Detection of apoptosis in nucleus pulposus. (A) TUNEL staining for apoptotic cells (green). The nuclei are labelled with DAPI (blue). Scale bar=20 μm. (B) Quantification of the nucleus pulposus cell apoptosis rate (n=5). Data are presented as the mean ± SD. **P<0.01 vs. sham group; $^{\#\#}$P<0.01 vs. control group. FGF-18, fibroblast growth factor 18.

IVD cells (26). FGF-18 has been identified as a powerful anabolic growth factor involved in cartilage homeostasis (27). The present study hypothesized that FGF-18 can protect against IVD degeneration, which was investigated using a lentivirus-mediated gene transfer approach in a rabbit annular needle puncture model.

In the NP *in vitro* model, overexpression of FGF-18 increased cell viability and inhibited the apoptosis induced by TBHP. To study the effect of FGF-18 *in vivo*, the transfection efficiency of FGF-18 overexpression lentivirus was first assessed by measuring the expression of Flag protein co-expressed with FGF-18. The data indicated that Flag was stably expressed 8 weeks after the operation. Histological examination indicated that local injection of FGF-18 overexpression lentivirus into the discs delayed the process of degeneration. In normal IVDs, anabolic factors promote the generation of PG and collagen, and catabolic factors inhibit the synthesis of the matrix to maintain a dynamic balance (28). A previous study reported that extracellular matrix degradation enzymes, such as MMPs and ADAMTSs, which are upregulated by proinflammatory cytokines, are characteristics of IVD degeneration (29). RT-qPCR was used to detect the expression of the catabolic indicators MMP-3 and ADAMTS-5 and demonstrated that their mRNA levels were increased in the control group. The expression level was decreased after FGF-18 intervention, suggesting that FGF-18 has an inhibitory effect on the synthesis of extracellular matrix degradation enzymes in IVD.

The apoptosis of NPs may play critical pathogenic roles in IVD degradation (30-32). A previous study showed that Bcl-2 overexpression in NPs prevented apoptotic cell death under serum-starved conditions (33). Importantly, another previous study reported that caspase-3 small interfering RNA attenuated Bcl-2 expression induced in rabbit IVD degeneration (34). These results indicate that inhibition of apoptosis of disc NPs may mitigate disc degeneration. Thus, in the present study, several apoptotic markers were quantified to evaluate the function of FGF-18 in NPs. The results of the western blot analysis indicated that the expression level of Bax was significantly reduced in the FGF-18 groups compared with in the control group, and the expression of Bcl-2 was significantly increased. Immunohistochemical analysis of cleaved caspase-3 showed that the percentage of cleaved caspase-3-positive cells was significantly increased in the model. Moreover, FGF-18 treatment reduced the expression of cleaved caspase-3. TUNEL staining demonstrated a similar result: The apoptotic index was decreased after FGF-18 treatment. Thus, apoptotic cell death of NPs was rescued by FGF-18 therapy in the present rabbit model of IVD degeneration.

The purpose of the present study was to preliminarily explore possible effects of the application of FGF-18 for the treatment of IVD degeneration. Using *in situ* hybridization technique, Ellsworth *et al* (14) found that FGF receptor (FGFR)18, FGFR3IIIc and FGFR2IIIc mRNAs were localized in chondrocytes of human articular cartilage, suggesting a potential role of FGFR2 or FGFR3 in FGF-18-mediated human articular cartilage homeostasis. In addition, FGFR can activate MAPK signaling pathways, with various downstream signaling cascades specific to the subtypes activated by FGFR (35). FGFR1-mediated MAPK activation leads to the activation of runt-related transcription factor 2 and ETS like-1 protein, and subsequently induces the expression of multiple MMPs, aggrecanases and leads to chondrocyte hypertrophy (36). FGFR3-mediated MAPK signaling could activate a different set of the downstream transcription factors, leading to chondroprotective effects (37). To date, the precise signaling pathway mediated by the FGFR3-FGF-18 axis in cartilage homeostasis is unknown. Thus, each part of the molecular mechanism requires investigation *in vivo* and *in vitro*. A comparison of the expression of extracellular matrix-degrading enzymes MMP-3 and ADAMTS-5 indicated that FGF-18 had anti-catabolic effects in IVD degeneration. Furthermore, the present data of the immunohistochemical analysis and TUNEL assay indicated that the protective effects were associated with inhibition of apoptosis in NPs.

In conclusion, the present study indicated that TBHP-induced apoptosis can be attenuated in FGF-18-treated NPs, and FGF-18 treatment can ameliorate puncture-induced IVD degeneration in rabbits. These findings suggested that a therapeutic strategy of FGF-18 application may be a promising treatment for IVD degeneration.

Acknowledgements

Not applicable.

Funding

The present study was supported by the Science-technology Program of Wenzhou Municipal Sci-Tech Bureau (grant no. 2020Y1553).

Availability of data and materials

The datasets used and/or analyzed during the current study are available from the corresponding author on reasonable request.

Authors' contributions

SL and CL searched the literature, designed the experiments and performed the experiments. SL analyzed, interpreted the data and wrote the manuscript. CL revised the manuscript. SL and CL confirmed the authenticity of all the raw data. Both authors have read and approved the final manuscript.

Ethics approval and consent to participate

All procedures and experimental operations were approved by the Animal Care and Use Committee of Wenzhou Medical University.

Patient consent for publication

Not applicable.

Competing interests

The authors declare that they have no competing interests.

References

1. Masuda K and An HS: Growth factors and the intervertebral disc. Spine J 4 (Suppl 6): S330-S340, 2004.

2. Kamali A, Ziadlou R, Lang G, Pfannkuche J, Cui S, Li Z, Richards RG, Alini M and Grad S: Small molecule-based treatment approaches for intervertebral disc degeneration: Current options and future directions. Theranostics 11: 27-47, 2021.
3. Cazzanelli P and Wuertz-Kozak K: MicroRNAs in intervertebral disc degeneration, apoptosis, inflammation, and mechanobiology. Int J Mol Sci 21: 3601, 2020.
4. Kim MJ, Lee JH, Kim JS, Kim HY, Lee HC, Byun JH, Lee JH, Kim NH and Oh SH: Intervertebral disc regeneration using stem cell/growth factor-loaded porous particles with a leaf-stacked structure. Biomacromolecules 21: 4795-4805, 2020.
5. Cui H, Zhang J, Li Z, Chen F, Cui H, Du X, Liu H, Wang J, Diwan AD and Zheng Z: Growth differentiation factor-6 attenuates inflammatory and pain-related factors and degenerated disc-induced pain behaviors in rat model. J Orthop Res 39: 959-970, 2021.
6. Hodgkinson T, Shen B, Diwan A, Hoyland JA and Richardson SM: Therapeutic potential of growth differentiation factors in the treatment of degenerative disc diseases. JOR Spine 2: e1045, 2019.
7. Clouet J, Fusellier M, Camus A, Le Visage C and Guicheux J: Intervertebral disc regeneration: From cell therapy to the development of novel bioinspired endogenous repair strategies. Adv Drug Deliv Rev 146: 306-324, 2019.
8. An JL, Zhang W, Zhang J, Lian LC, Shen Y and Ding WY: Vitamin D improves the content of TGF-β and IGF-1 in intervertebral disc of diabetic rats. Exp Biol Med (Maywood) 242: 1254-1261, 2017.
9. Chen S, Liu S, Ma K, Zhao L, Lin H and Shao Z: TGF-β signaling in inter-ertebral disc health and disease. Osteoarthritis Cartilage 27: 1109-1117, 2019.
10. Xu Z, Zhou X and Chen G: Expression and mechanism of interleukin 1 (IL-1), interleukin 2 (IL-2), interleukin 8 (IL-8), BMP, fibroblast growth factor 1 (FGF1), and insulin-like growth factor (IGF-1) in lumbar disc herniation. Med Sci Monit 25: 984-990, 2019.
11. Ellman MB, An HS, Muddasani P and Im HJ: Biological impact of the fibroblast growth factor family on articular cartilage and intervertebral disc homeostasis. Gene 420: 82-89, 2008.
12. Ellman MB, Yan D, Ahmadinia K, Chen D, An HS and Im HJ: Fibroblast growth factor control of cartilage homeostasis. J Cell Biochem 114: 735-742, 2013.
13. Häckel S, Zolfaghar M, Du J, Hoppe S, Benneker LM, Garstka N, Peroglio M, Alini M, Grad S, Yayon A and Li Z: Fibrin-hyaluronic acid hydrogel (RegenoGel) with fibroblast growth factor-18 for in vitro 3D culture of human and bovine nucleus pulposus cells. Int J Mol Sci 20: 5036, 2019.
14. Ellsworth JL, Berry J, Bukowski T, Claus J, Feldhaus A, Holderman S, Holdren MS, Lum KD, Moore EE, Raymond F, *et al*: Fibroblast growth factor-18 is a trophic factor for mature chondrocytes and their progenitors. Osteoarthritis Cartilage 10: 308-320, 2002.
15. Moore EE, Bendele AM, Thompson DL, Littau A, Waggie KS, Reardon B and Ellsworth JL: Fibroblast growth factor-18 stimulates chondrogenesis and cartilage repair in a rat model of injury-induced osteoarthritis. Osteoarthritis Cartilage 13: 623-631, 2005.
16. Muresanu C, Somasundaram SG, Vissarionov SV, Gavryushova LV, Nikolenko VN, Mikhaleva LM, Kirkland CE and Aliev G: Hypothetical role of growth factors to reduce intervertebral disc degeneration significantly through trained biological transformations. Curr Pharm Des: Oct 18, 2020 (Epub ahead of print).
17. Yue B, Lin Y, Ma X, Xiang H, Qiu C, Zhang J, Li L and Chen B: Survivin-TGFB3-TIMP1 gene therapy via lentivirus vector slows the course of intervertebral disc degeneration in an in vivo rabbit model. Spine (Phila Pa 1976) 41: 926-934, 2016.
18. Mobasheri A and Richardson SM: Cell and gene therapy for spine regeneration: Mammalian protein production platforms for overproduction of therapeutic proteins and growth factors. Neurosurg Clin N Am 31: 131-139, 2020.
19. National Research Council (US) Institute for Laboratory Animal Research: Guide for the Care and Use of Laboratory Animals. National Academies Press (US), Washington, DC, 1996.
20. Giry-Laterrière M, Verhoeyen E and Salmon P: Lentiviral vectors. Methods Mol Biol 737: 183-209, 2011.
21. Masuda K, Aota Y, Muehleman C, Imai Y, Okuma M, Thonar EJ, Andersson GB and An HS: A novel rabbit model of mild, reproducible disc degeneration by an anulus needle puncture: Correlation between the degree of disc injury and radiological and histological appearances of disc degeneration. Spine (Phila Pa 1976) 30: 5-14, 2004.
22. Imai Y, Okuma M, An HS, Nakagawa K, Yamada M, Muehleman C, Thonar E and Masuda K: Restoration of disc height loss by recombinant human osteogenic protein-1 injection into intervertebral discs undergoing degeneration induced by an intradiscal injection of chondroitinase ABC. Spine (Phila Pa 1976) 32: 1197-1205, 2007.
23. Livak KJ and Schmittgen TD: Analysis of relative gene expression data using real-time quantitative PCR and the 2(-Delta Delta C(T)) method. Methods 25: 402-408, 2001.
24. Choi UY, Joshi HP, Payne S, Kim KT, Kyung JW, Choi H, Cooke MJ, Kwon SY, Roh EJ, Sohn S, *et al*: An injectable hyaluronan-methylcellulose (HAMC) hydrogel combined with Wharton's Jelly-derived mesenchymal stromal cells (WJ-MSCs) promotes degenerative disc repair. Int J Mol Sci 21: 7391, 2020.
25. Nishida K, Kang JD, Gilbertson LG, Moon SH, Suh JK, Vogt MT, Robbins PD and Evans CH: Modulation of the biologic activity of the rabbit intervertebral disc by gene therapy: An in vivo study of adenovirus-mediated transfer of the human transforming growth factor beta 1 encoding gene. Spine (Phila Pa 1976) 24: 2419-2425, 1999.
26. Vo NV, Hartman RA, Yurube T, Jacobs LJ, Sowa GA and Kang JD: Expression and regulation of metalloproteinases and their inhibitors in intervertebral disc aging and degeneration. Spine J 13: 331-341, 2013.
27. Xie Y, Zinkle A, Chen L and Mohammadi M: Fibroblast growth factor signalling in osteoarthritis and cartilage repair. Nat Rev Rheumatol 16: 547-564, 2020.
28. Adams MA and Roughley PJ: What is intervertebral disc degeneration, and what causes it? Spine (Phila Pa 1976) 31: 2151-2161, 2006.
29. Chung SA, Khan SN and Diwan AD: The molecular basis of intervertebral disk degeneration. Orthop Clin North Am 34: 209-219, 2003.
30. Heyde CE, Tschoeke SK, Hellmuth M, Hostmann A, Ertel W and Oberholzer A: Trauma induces apoptosis in human thoracolumbar intervertebral disc. BMC Clin Pathol 6: 5, 2003.
31. Rannou F, Lee TS, Zhou RH, Chin J, Lotz JC, Mayoux-Benhamou MA, Barbet JP, Chevrot A and Shyy JY: Intervertebral disc degeneration: The role of the mitochondrial pathway in annulus fibrosus cell apoptosis induced by overload. Am J Pathol 164: 915-924, 2004.
32. Lin X and Lin Q: μiRNA-495-3p attenuates TNF-α induced apoptosis and inflammation in human nucleus pulposus cells by targeting IL5RA. Inflammation 43: 1797-1805, 2020.
33. Sudo H and Minami A: Regulation of apoptosis in nucleus pulposus cells by optimized exogenous Bcl-2 overexpression. J Orthop Res 28: 1608-1613, 2010.
34. Yamada K, Sudo H, Iwasaki K, Sasaki N, Higashi H, Kameda Y, Ito M, Takahata M, Abumi K, Minami A, *et al*: Caspase 3 silencing inhibits biomechanical overloade induced intervertebral disk degeneration. Am J Pathol 184: 753-764, 2014.
35. Mao P, Cohen O, Kowalski KJ, Kusiel JG, Buendia-Buendia JE, Cuoco MS, Exman P, Wander SA, Waks AG, Nayar U, *et al*: Acquired FGFR and FGF alterations confer resistance to estrogen receptor (ER) targeted therapy in ER^+ metastatic breast cancer. Clin Cancer Res 26: 5974-5989, 2020.
36. Yan D, Chen D and Im HJ: Fibroblast growth factor-2 promotes catabolism via FGFR1-Ras-Raf-MEK1/2-ERK1/2 axis that coordinates with the PKCδ pathway in human articular chondrocytes. J Cell Biochem 13: 2856-2865, 2012.
37. Davidson D, Blanc A, Filion D, Wang H, Plut P, Pfeffer G, Buschmann MD and Henderson JE: Fibroblast growth factor (FGF) 18 signals through FGF receptor 3 to promote chondrogenesis. J Biol Chem 280: 20509-20515, 2005.